Mar Geophys Res (2009) 30:73–84
DOI 10.1007/s11001-009-9068-y

ORIGINAL RESEARCH PAPER

Submarine structures in the Gulf of İzmit, based on multichannel seismic reflection and multibeam bathymetry

Hülya Kurt · Esra Yücesoy

Received: 16 August 2008 / Accepted: 25 May 2009 / Published online: 12 June 2009

Abstract Multichannel seismic reflection and multibeam bathymetry data were used to study the active tectonic and syn-tectonic stratigraphic setting of the Gulf of İzmit in the Marmara Sea (Turkey). The gulf and its near surroundings are deformed by the northern strand of the dextral North Anatolian Fault. Three connected basins of the gulf, the western (Darıca), central (Karamürsel) and eastern (Gölcük) basins are formed by active faults, as observed in the stacked and migrated seismic sections, as well as the bathymetry map. The main branch and its surrounding sedimentary strata are confined by normal faults to the north and south. These normal faults converge at depth towards the main fault, forming a negative flower structure in the gulf. The average maximum sedimentation rate is 0.4 mm/year according to the three most recent seismo-stratigraphic units that are located to the south of the main fault branch within the central basin. A 20° south-dipping major discontinuity along the northern shoreline of the gulf represents the top of Paleozoic basement.

Keywords Sea of Marmara · Gulf of İzmit · North Anatolian Fault · Multichannel seismic reflection data

Introduction

The Gulf of İzmit is located in the eastern part of Marmara Sea. It is, on average, 50 km long and 10 km wide (Fig. 1). The northern strand of the North Anatolian Fault enters the Marmara Sea through the Gulf of İzmit. The North Anatolian Fault is an E–W trending right-lateral strike-slip transform fault running across northern Turkey with a length of ~1,600 km (Şengör et al. 1985; Şaroğlu 1988). The fault zone is one of the most tectonically active regions of the world. The mechanics of strike-slip faulting and its associated structures have been extensively studied (Tchalenko 1970; Wilcox et al. 1973; Wernike and Burchfiel 1982; Sylvester 1988). Eight westward-progressing fault ruptures along the North Anatolian Fault have caused destructive earthquakes (Barka 1996; Stein et al. 1997), the last two of which occurred on 17 August 1999 ($M_w = 7.4$) and 12 November 1999 ($M_w = 7.2$). Stress triggering has been proposed as the cause of the westward progression of earthquakes along the North Anatolian Fault, and has increased the probability of a large earthquake on the western segment of the fault (Barka 1999; Parsons et al. 2000). The Gulf of İzmit is a key location for understanding the geometry of the North Anatolian Fault, because it also includes the offshore continuation of the August 17th fault rupture.

Three connected basins, the western (Darıca), central (Karamürsel) and eastern (Gölcük) basins, form the Gulf of İzmit (Fig. 2). The central basin is connected to the other basins by two shallow sills located north of the Hersek Peninsula and north of Gölcük at about 55 and 38 m water depths, respectively. The evolution of the Gulf of İzmit has been studied by various groups (Şengör et al. 1999; Gökaşan et al. 2001; Alpar and Yaltırak 2002; Kuşçu et al. 2002; Polonia et al. 2004; Cormier et al. 2006). It is generally accepted that the geological structures in the gulf are mostly formed by deformation related to the North Anatolian Fault, but their distribution and interpretation differ. Conventional bathymetry, coastal morphology, coarse grids of shallow seismic lines, and measured seismicity have been used to infer the geometry of the active faults in

H. Kurt (✉) · E. Yücesoy
Department of Geophysics, Istanbul Technical University, 34390 Maslak, Istanbul, Turkey
e-mail: kurt@itu.edu.tr

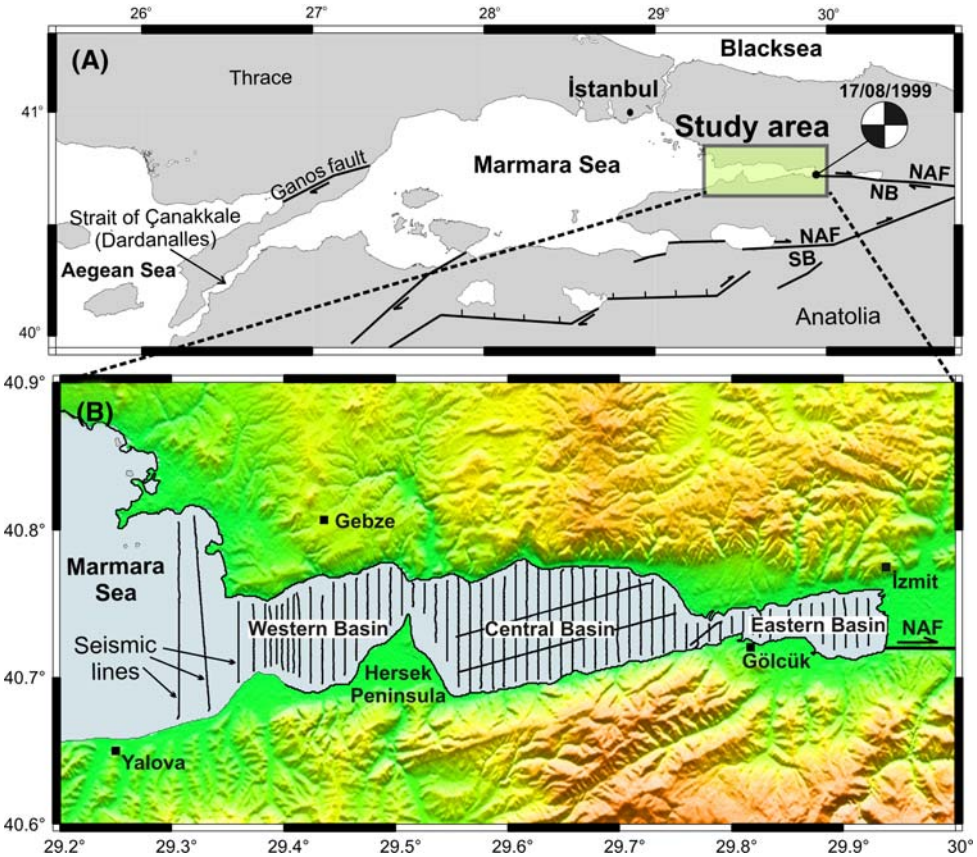

Fig. 1 **a** Location map of the study area. Active faulting in Marmara regions is modified after Barka (1997). NAF, North Anatolian Fault splays into a main northern branch (*NB*) and a southern branch (*SB*). *Black dot* indicates the epicenter of the 1999 Gölcük-Kocaeli earthquake, the focal mechanism for it being by Taymaz (1999). **b** Location of the seismic reflection lines and elevation model of the area. The total length of seismic lines is 345 km. Topography data are compiled from The Shuttle Radar Topography Mission, SRTM (http://www2.jpl.nasa.gov/srtm) and mapped by using Generic Mapping Tools, GMT software programming (Wessel and Smith 1998)

the Gulf of İzmit, which has been interpreted as a series of negative flower structures (Gökaşan et al. 2001; Alpar and Yaltırak 2002; Kuşçu et al. 2002). Polonia et al. (2004) proposed that the three basins in the gulf are depressions, bounded by short, en échelon extensional and strike-slip segments, forming a sequence of pull-apart basins. Cormier et al. (2006) noted that the main fault follows the axis of the gulf in a dominantly E–W direction with a few minor bends and that dip-slip movement is accommodated along the transform fault. Stratigraphic analysis of shallow seismic sections and borehole data has provided additional information on past marine, lacustrine, and fluvial conditions in the Gulf of Izmit (Gökaşan et al. 2001; Alpar and Yaltırak 2002; Kuşçu et al. 2002; Çağatay et al. 2003; Polonia et al. 2004).

In a recent study, high-resolution seismic reflection data correlated with borehole data indicate that the stratigraphy of the Gulf of İzmit consists of three distinct depositional sequences formed in response to middle Pleistocene-Holocene sea-level changes (Okyar et al. 2008). Okyar et al. (2008) interpreted two distinct fault systems in the gulf: The main fault system extending roughly in an E–W direction along the gulf is an active right lateral strike-slip fault with a normal component. The secondary faults are normal faults striking in different directions and are identified as being both active and inactive.

The main purpose of this study is to investigate the deep structural and stratigraphic features of the Gulf of İzmit using deep-penetration multichannel seismic data, as well as multibeam bathymetry and onshore geological data. Previous studies used very shallow-penetrating seismic data that was too limited to observe the active faults at depths greater than about 250 m (Gökaşan et al. 2001; Alpar and Yaltırak 2002; Kuşçu et al. 2002; Çağatay et al. 2003; Polonia et al. 2004; Cormier et al. 2006). Şengör et al. (1999) interpreted single-channel sections of the same data used in this study. However, signal to noise ratio, reflector continuity, vertical and horizontal resolution of the single-channel seismic sections were not as good quality as the multichannel processed seismic reflection sections that were generated and interpreted in this study.

Onshore geology

The main branch of the North Anatolian Fault enters the Sea of Marmara from the eastern part of the Gulf of İzmit (Fig. 3a). According to Alpar and Yaltırak (2002), the onshore faults are developed oblique to the main fault and are divided into three groups: (a) ENE-WSW trending right-lateral oblique faults developed under a dextral shear regime (Yalova and Karamürsel Faults) (b) NW-SE

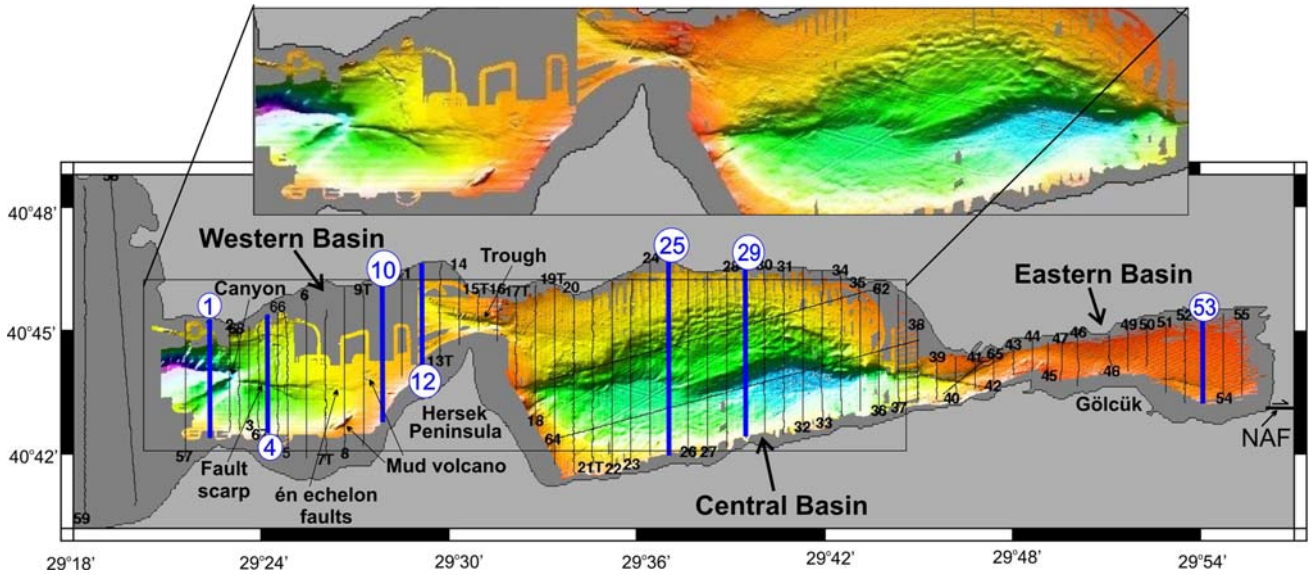

Fig. 2 Multibeam bathymetric relief map of the Gulf of İzmit and location of seismic lines. Three main basins, western, central and eastern basins are shaped by the northern branch of the NAF. *Upper picture* shows focused view of the western and the central basins. The multibeam data combined from R/V expeditions MARMARA 2000 of the R/V Odin Finder, MARMARA 2001 of the R/V Urania and Turkish Department of Navigation, Hydrography and Oceanography (SHOD). Bold seismic lines numbered in *circular labels* show seismic sections given in the paper. NAF indicates North Anatolian Fault. Generic Mapping Tools (*GMT*) software programming (Wessel and Smith 1998) is used for mapping with artificial sun illumination from the NW

trending extensional faults such as Orhangazi, Termal and Kavaklı (Gölcük) Faults and (c) small scale NNE-SSW trending left lateral faults that are usually found in the western Armutlu Peninsula.

The main stratigraphic units in the area are the Yalova, Samanlıdağ and Marmara Formations (Emre et al. 1998; Alpar and Yaltırak 2002; Fig. 3b). The Yalova Formation has a great extent on the Armutlu Peninsula where it includes the Kılınç and Yalakdere members. Kılınç Member is ~200-m-thick, upper Miocene-lower Pliocene (Emre et al. 1998) siliciclastic succession, which rests unconformably over basement rocks. The Yalakdere Member consists of ~200-m-thick cemented sandstones, siltstones and cream-colored marls of early Pliocene age (Emre et al. 1998), resting on the Kılınç Member with vertical and lateral transitions. The Samanlıdağ formation consists of 20–50 m-thick coarse sandstone and conglomerate lenses of upper Pliocene-lower Pleistocene age and represents braided river and alluvial fan deposition. According to Alpar and Yaltırak (2002), the Marmara formation consists of transgressive sandstone, calcareous sandstones with abundant bivalves, and occasional conglomerate interbeds of middle to upper Pleistocene age. The thickness of the Marmara formation ranges from a few tens of centimeters up to 37 m. There are three large alluvial fans covering the coastal areas; the Çatal, Hersek and Gölcük deltas (Fig. 3a).

Data acquisition and processing

Multichannel seismic reflection data were collected in cooperation with the Directorate of Mineral Research and Exploration of Turkey (MTA) and the Department of Geophysics, Istanbul Technical University (ITU). Seismic profiles were acquired with R/V *MTA Sismik-1* along 63 lines totaling 348 km in September 1999, just after the 17 August 1999 earthquake (Fig. 1b). Most of the seismic lines are oriented in an N–S direction with a line interval of 1 km except for a few lines in the west where the line interval is 0.5 km (Fig. 1b). Although a Differential Global Positioning System (DGPS) was operated during data acquisition, navigation was carried out using the standard GPS mode of the system because of poor differential signal reception from the base station. The energy source consisted of one or two generator-injector (GI) air guns each of 45 cu in volume. The number of channels was 18 during acquisition. Both the receiver group interval and near offset are 12.5 m. Shot intervals were 6.25 or 12.5 m. These parameters provided 9- or 18-fold common-depth-point (CDP). The sampling interval and record length were 1 and 1,500 ms, respectively during recording.

The seismic data were processed with *Focus* (5.0) software in the geophysical data processing laboratory of the Department of Geophysics, ITU. A conventional data processing stream was applied to the data as follows: data

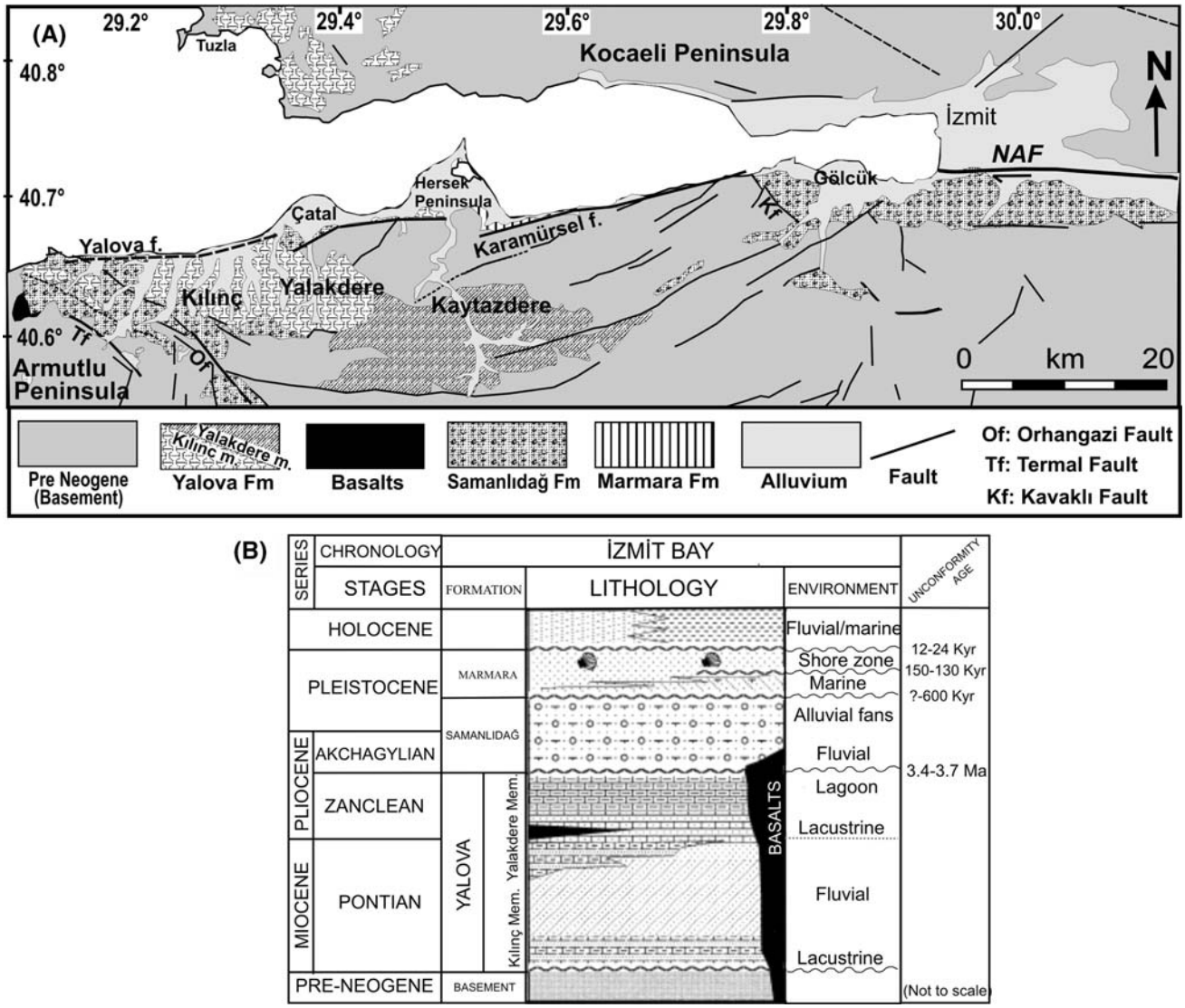

Fig. 3 **a** Geological map of gulf of İzmit and surroundings modified from Alpar and Yaltırak (2002). The main branch of the North Anatolian Fault (*NAF*) enters to the sea from the easternmost part of the gulf of Izmit. There is other group of onshore faults developed oblique to the master fault (NAF). **b** Generalized stratigraphic section of the study area modified from Alpar and Yaltırak (2002) shows the Yalova, Samanlıdağ and Marmara Formations deposited in lacustrine to fluvial/marine environments related to transgressive/regressive regimes

transcription, in-line geometry definition, editing, CDP sorting, gain correction, band-pass filtering, velocity analysis, normal-move-out correction, muting, stacking, signal shaping deconvolution, band-pass filtering, automatic gain control, and poststack finite-difference time migration. Thus, we obtained stacked and migrated seismic sections that for the first time cover the İzmit Gulf. These new seismic sections have better signal to noise ratio, reflection continuity and reflector geometry compared to the single-channel seismic sections interpreted by Şengör et al. (1999). Although repeated attempts were made to eliminate bottom multiples with detailed velocity analysis and post-stack predictive deconvolution, we were not successful in suppressing them significantly.

R/V *Odin Finder* and R/V *Urania* collected multibeam bathymetric data in western and central basins of the gulf in 2000 and 2001, respectively (Polonia et al. 2004; Cormier et al. 2006). These areas were surveyed with three multibeam systems, the Simrad EM300 (30 kHz), EM3000 (300 kHz) and portable SeaBeam 1180 (180 kHz) multibeam. These systems provide about 10 cm vertical resolution and a mean footprint of a few square meters over the shelf. Survey localities were positioned by a DGPS satellite navigation system. The bathymetric data of the eastern gulf were acquired in 1999 by the Department of Navigation, Hydrography and Oceanography of the Turkish Navy (SHOD). The western and central parts were compiled in Cormier et al. (2006). These two gridded bathymetric data

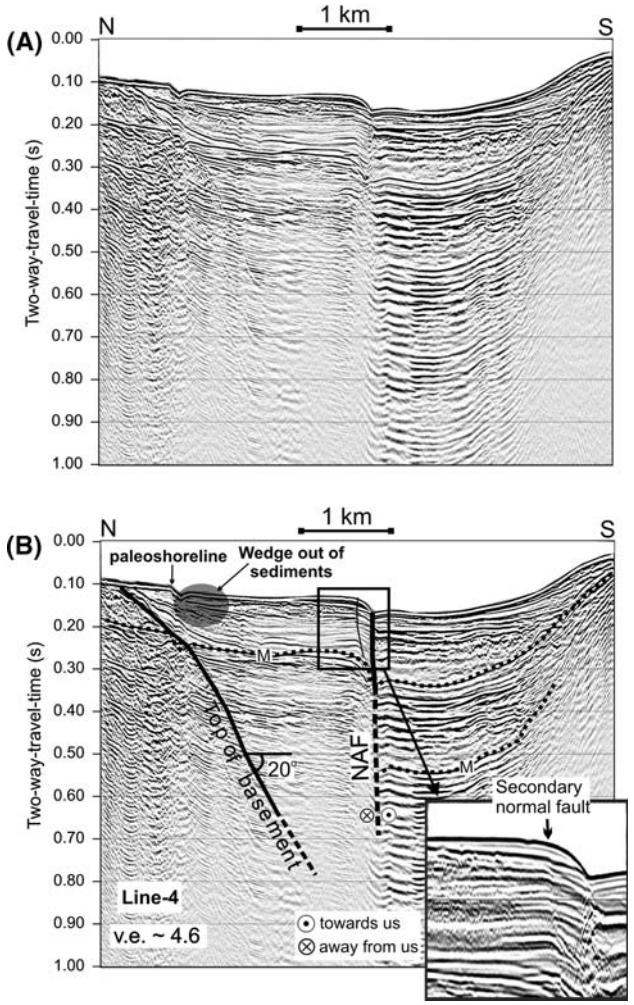

Fig. 4 **a** Time-migrated seismic Section-4 **b** interpreted section. The vertical feature in the middle part of the section is interpreted as the North Anatolian Fault (NAF) which is correlated with the bathymetry. The south dipping discontinuity on the northern side shows the top of the basement with a 20° southward dip. *M* sea bottom multiple, *v.e* vertical exaggeration. The v-shaped structure is the paleoshoreline located at 85 m below the present day sea level (Çağatay et al. 2003; Polonia et al. 2004). *Inset* shows secondary normal faults close to the main fault

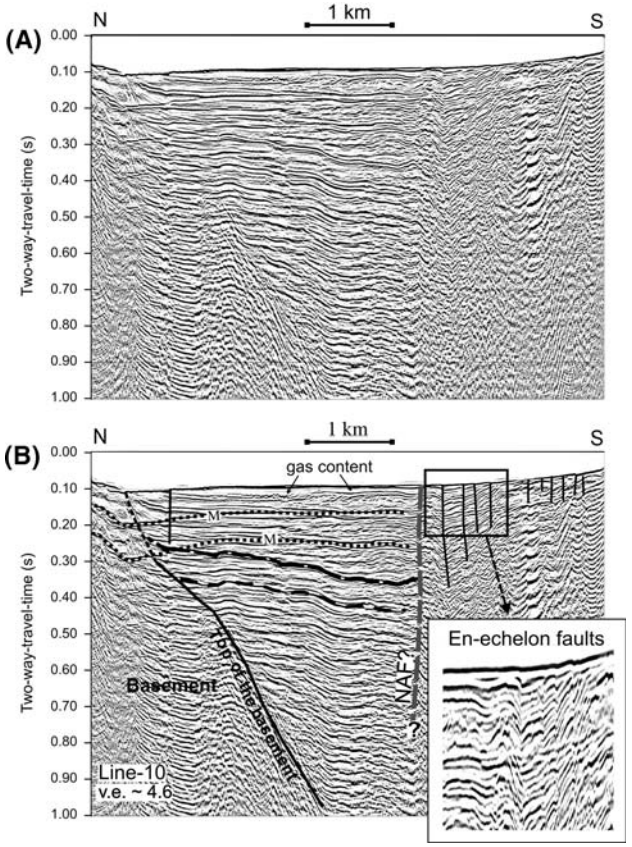

Fig. 5 **a** Time-migrated seismic Section-10 **b** interpreted section. To the south, en échelon faults reflected to the bathymetry are observed. The faults cutting the sea bottom as well as younger sediments are clearly seen in the *inset* figure. The south dipping northern discontinuity is still seen and it has an undulation between 0.4 and 0.5 s. *M* two sea bottom multiples, *v.e* vertical exaggeration

have been merged to map the bathymetry of the gulf, from which traces of the active faults can be inferred.

Seismic stratigraphy and structural observations

Here we present seismic sections in order to discuss the structural and stratigraphic features of active tectonics in the gulf from west to east. The location of the seismic lines is given in Fig. 2. Time-migrated seismic Sect. 4 shows the general structural characteristics of the western basin (Fig. 4). A vertical discontinuity in the middle part of the seismic section can be traced confidently down to about 0.35 s two-way travel time, corresponding to ~350 m. This discontinuity, which has more than 30 m vertical offset at the seafloor, is one of the main branches of the North Anatolian Fault in the gulf. This fault cannot be seen clearly deeper than 0.35-s because the seabed multiples cover the primary reflections. The fault forms an E–W trending scarp in the bathymetry (Fig. 2). To the north of this main fault branch some secondary normal faults that cut the uppermost sediments are visible in the seismic section (inset of Fig. 4). A v-shaped trough on the sea bottom with 14 m of vertical relief is observed in the northern part of the same seismic section. The northern bank of this trough is higher than the southern bank and sedimentary units wedge out below the sea bottom to the south of this v-shaped structure. This trough is also observed on Sect. 66 to the east of Sect. 4 (Fig. 2) and can be traced to the north and south on the bathymetry.

Previous sediment core analyses over similar morphological features suggest that the v-shaped structure is a paleoshoreline located at 85 m below the present day sea level (Çağatay et al. 2003; Polonia et al. 2004). The depth

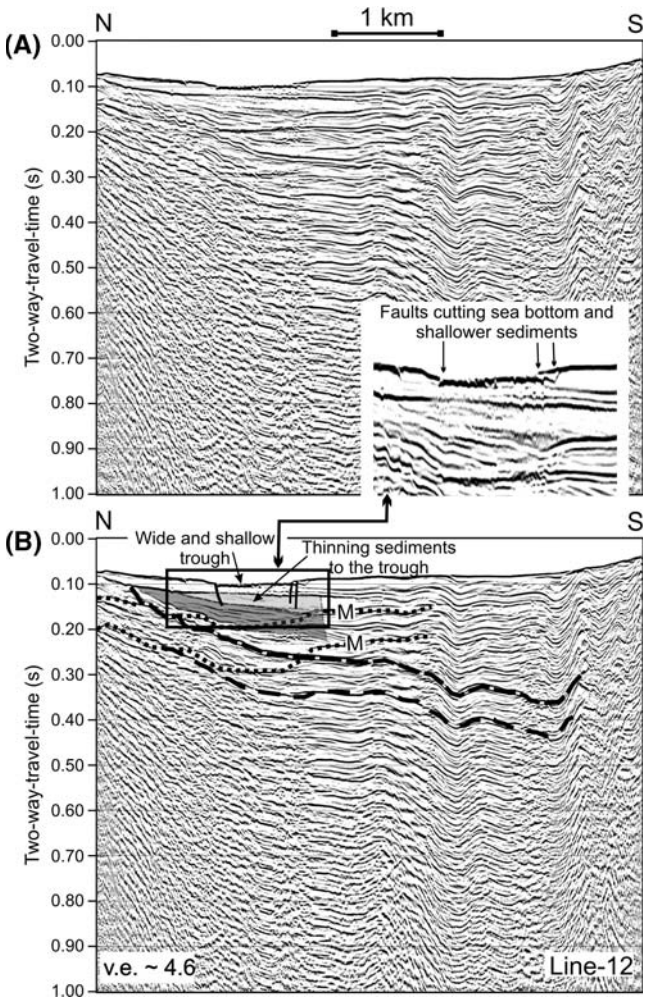

Fig. 6 **a** Time-migrated seismic Section-12 **b** interpreted section. The section is located across the sill area between western and central basins of the gulf. Note that the surficial sedimentary sequence pinches toward the wide, shallow trough, from both sides. The two border of the trough is faulted and the northern border of this structure has NW-SE lineament in the map view. Wavy shape south dipping northern discontinuity reaches to the south tip of the section. *M* sea bottom multiple, *v.e* vertical exaggeration

of the paleo-shoreline in the gulf as interpreted by Cormier et al. (2006) was actually closer to 92 m.

A steeply south-dipping reflector is observed to the north of the v-shaped trough, which can be traced from the seafloor to 0.65 s two-way travel-time (Fig. 4). Based on the average seismic velocity derived from our velocity analysis (about 2,000 m/s up to 1 s two-way travel time), we calculate the true dip of that reflector to be about 20°. This reflector is observed in many seismic sections in the west and central basins of the gulf (between Sects. 4 and 34). It crops out in some places at the seafloor and we interpret the reflector to represent the top of the basement along the northern margin of the gulf.

In the eastern part of the western basin, some relatively small-scale and shorter normal faults are observed in the time-migrated seismic sections (Fig. 5). These are en échelon faults cutting the seafloor, as well as younger sediments as seen in the inset of Fig. 5. The faults trend WNW-ESE, as seen in the bathymetry map and join the main fault trace in the west. A vertical discontinuity just north of the en échelon faults can be related to the main branch of the North Anatolian Fault. The south-dipping discontinuity observed in the western basin is also seen in this seismic section and it has a slope-break between 0.4 and 0.5 s. Two other south-dipping reflectors with shallower dip angles and wavy, irregular shapes occur at around 0.25 and 0.35 s two-way travel time (Fig. 5). These extend about 3 km from north to south and are cut by the North Anatolian Fault and the en échelon fault system to the south. The sill between the western and central basins of the gulf (between Sects. 11 and 17T on Fig. 2) shows relatively flat seafloor morphology except for a trough in the middle of the section. The sedimentary sequences observed in the seismic sections thin towards this trough (Fig. 6). The two borders of this trough appear to be faulted and the northern side of this trough trends in a WNW-ESE direction, as seen in the bathymetry. The two shallow, south-dipping reflectors observed on other seismic sections are also present in the sill area, crossing the bottom multiples between 0.3 and 0.4 s two-way travel time (Fig. 6).

The central basin contains the deepest seafloor in the gulf at 205 m depth and two deep troughs, lenticular in

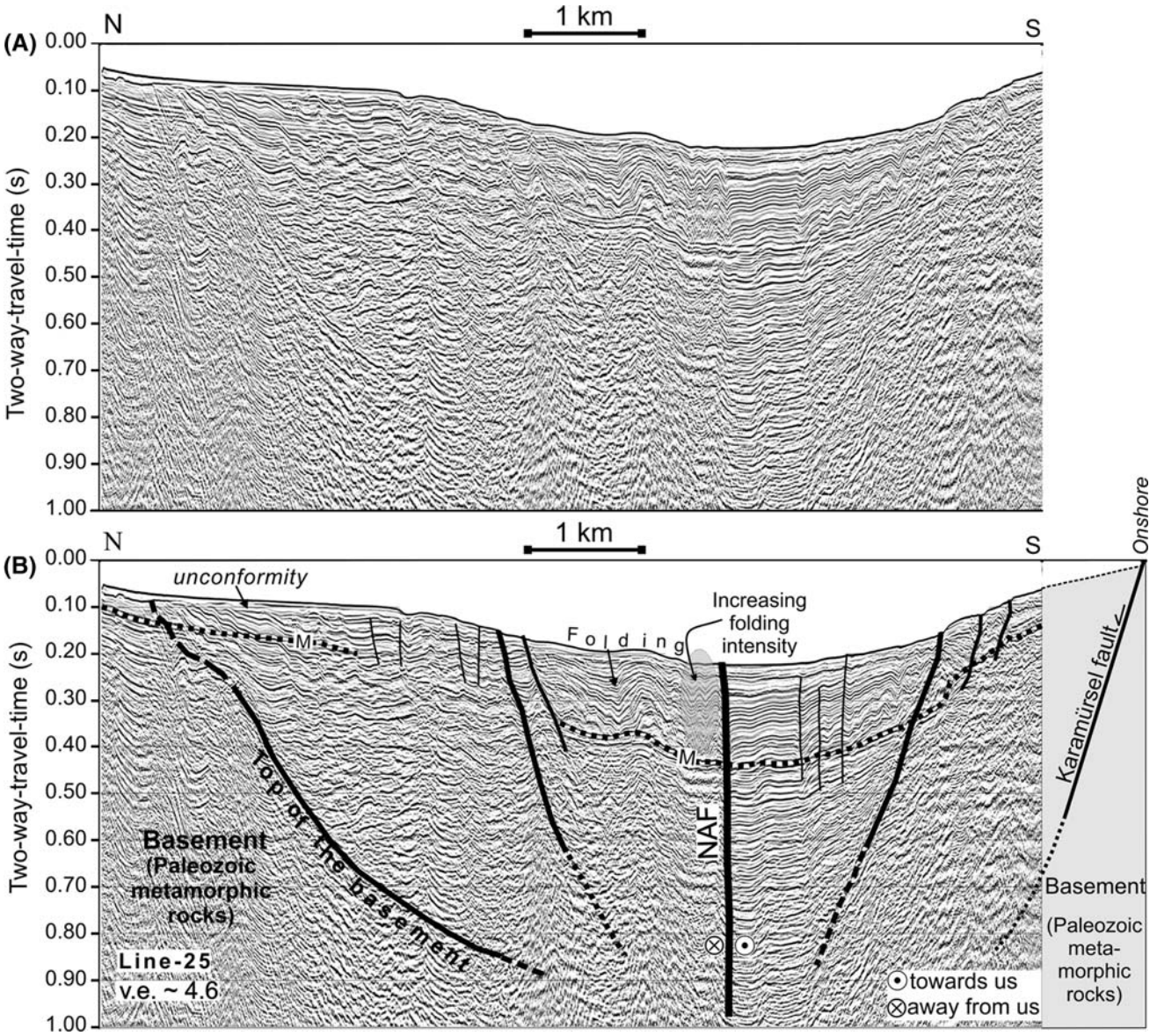

Fig. 7 **a** Time-migrated seismic Section-25 **b** interpreted section. The section shows general structural characteristics of the central basin. The NAF is seen as a vertical discontinuity separating two different seismic units. A *folded strata* is seen to the north of the North Anatolian Fault (NAF), while the seismic character south of the fault suggests an extensional regime. The southern margin of the section is extrapolated to onshore geology based on the study of Alpar and Yaltırak (2002). *M* sea bottom multiple, *v.e* vertical exaggeration

plan view and trending E–W (Fig. 2). Section 25 (Fig. 7) shows the typical setting of the central basin. The prominent vertical discontinuity in the middle of the section is interpreted to correspond to the main branch of the North Anatolian Fault. This fault separates two distinct domains: folded beds to the north and syn-sedimentary less deformed sequences to the south. To the south of this fault, relatively thick, sub-parallel sedimentary strata are cut by secondary subvertical normal faults, which can be traced from the sea bottom to 0.5 s two-way travel-time. The thickness of the sedimentary sequences increases towards the North Anatolian Fault, reflecting fault activity. Note that strata are more intensely folded just north of the fault. Folded sequences north of the fault and the sub-parallel sequences south of the fault are bounded by south-dipping and north-dipping faults, respectively. These faults, which are interpreted from the terminations of stacked reflectors, can be traced from the sea bottom to 0.6 s depths and converge toward each other, defining a bowl-shape structure. In the north of the section, the top of basement is also clearly identified.

In the eastern part of the gulf, the seafloor shows a relatively shallow and flat bathymetry. The sediments below the seafloor are thinner than as in the case of the

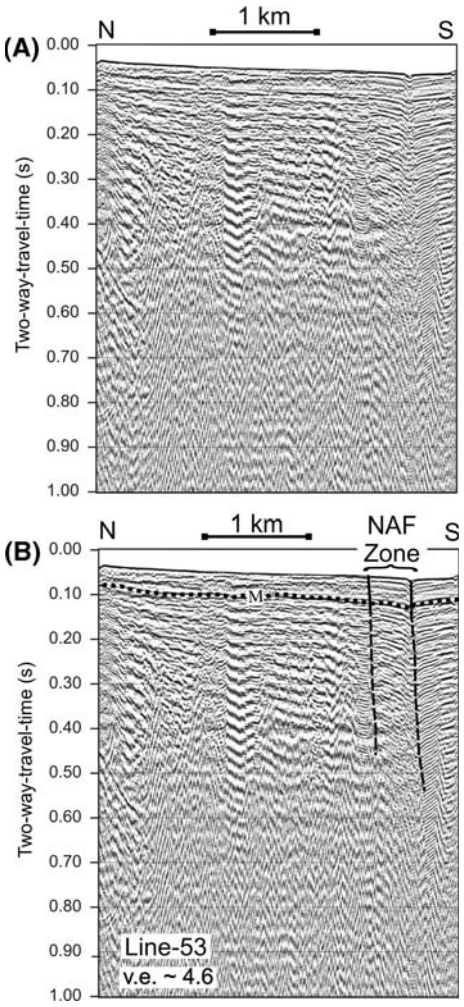

Fig. 8 **a** Time-migrated seismic Section-53 **b** interpreted section. In the eastern basin of the gulf, the seafloor is shallow and the sediments below the seafloor relatively thin comparing with western and central basins. The two parallel faults are well correlated with the lineaments observed in the multibeam bathymetry (Fig. 2). *M* sea bottom multiple, *v.e* vertical exaggeration. Strong sea bottom multiples due to the shallow seafloor make it difficult to observe the fault geometry in the deeper parts of the sections

western and central basins (Fig. 8). Strong sea bottom multiples cover all sections of the shallower eastern basin. However, the main fault is still observed in the upper part of the seismic sections. The bathymetric lineament helps to trace the fault in the section as explained in the following section.

Discussion

The structural map constructed from interpretation of the migrated seismic reflection sections and the bathymetry of the Gulf of İzmit is shown in Fig. 9. The main branch of the North Anatolian Fault extends mainly E–W and must accommodate dip-slip along those parts that can be traced as scarps in the bathymetry. Here we discuss the characteristics of the North Anatolian Fault in the Gulf of İzmit separately for each of the basins. Along the northern shoreline of the gulf, a south-dipping major discontinuity is followed (Figs. 4, 5, 7). The two reflectors seen on Sects. 10 and 12 (Figs. 5, 6) are interpreted as interfaces within the thick sedimentary strata developed over this major interface. In map view, the surface trace of this seismic discontinuity related a major interface is mainly parallel to the northern coast (Fig. 9). We interpret this major seismic discontinuity as corresponding to the top of basement in the Kocaeli Peninsula and consisting of Paleozoic rocks (Okay et al. 1994). Alternatively, the south dipping structure observed in our seismic sections may be an offshore extension of the Yarımca Fault (Fig. 9). The Yarımca Fault on the north shore of the gulf is an E–W trending fault that plunges underwater near 29°42′E (Fig. 9). In contrast, the south-dipping reflector does not offset the shallowest reflectors above a distinct unconformity (labeled in Fig. 7).

Western Basin

The main fault in the western basin follows an E–W bathymetric lineament. The seafloor slopes that define that lineament are <6° (Cormier et al. 2006). An E–W trending submarine canyon connects the western basin to the 1,200-m-deep Çınarcık Basin of the Marmara Sea (Fig. 2). To the west, the fault extends along the southern slope of the canyon and connects to the main fault in the Marmara Sea. To the east, the canyon sharply bends to the south, but the fault continues in an E–W direction and changes from a single strand to en échelon geometry. The North Anatolian Fault in the western part extends along the southern side of the canyon and forms a zone that separates relatively thick sediments on both sides (Fig. 10). In this area sediments on each side are faulted and folded as a result of the strike-slip movements of the fault zone. Further east in the western basin, as shown in seismic Sect. 4 (Fig. 4), folded sediments are also seen along the vertical fault surface forming an m-shaped surface on the sea bottom. In the western basin the canyon and the North Anatolian Fault are bordered by faults from south and north (Figs. 9, 10). These faults are observed at the seafloor, as well as in the underlying sediments. Their continuity, however, is not followed clearly on the adjacent seismic lines.

Despite the lack of seismic and bathymetric data along the coast of the Hersek Peninsula, the North Anatolian Fault is interpreted as continuing through the peninsula, as shown by dashed line in Fig. 9. The seismic appearance of the North Anatolian Fault in the west part of Hersek Peninsula has a distinctive character (Figs. 5, 6). Here the North Anatolian Fault does not show a sharp lineament in bathymetry and it does not show a clear vertical seismic

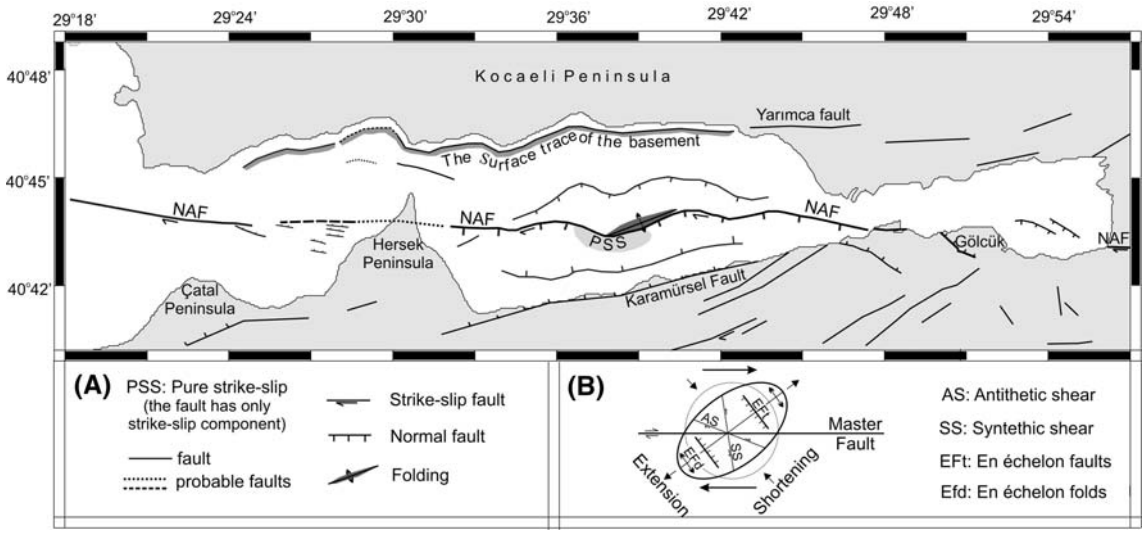

Fig. 9 Fault interpretation of the Gulf of İzmit constructed from the interpreted seismic sections. The North Anatolian Fault (NAF) mainly follows an EW direction and is associated in places with normal displacement that correlates with lineaments in the bathymetry. Secondary E–W trending faults are located at the border of the deeper part of the central basin. At the northern shoreline of the gulf a south dipping structure related to the top of basement is present. En échelon faults are observed just west of the Hersek Peninsula. The faults on land area are from Alpar and Yaltırak (2002) and Emre et al. (2003). Other geological features on the land area can be seen in Fig. 3. **a** Explanations for the figure. **b** Strain ellipse for deformation from Wilcox et al. (1973)

discontinuity in the sections as in the rest of the gulf. There is a WNW-ESE trending en échelon fault pattern, which can be compared to Riedel shear (R) fractures (Figs. 5, 9). Cormier et al. (2006) also proposed a Riedel shear interpretation based on the same bathymetry data. North-dipping en échelon faults cause back tilting of the beds because of normal faulting, i.e., rotation of both fault planes and beds, possibly due to an extensional component along the strike-slip fault (inset of Fig. 5; Wernike and Burchfiel 1982). To the north of the en échelon faults in Fig. 5, a vertical discontinuity extending from the seafloor to the deeper parts should indicate the presence of North Anatolian Fault because it cuts the thick sediments developed overlying the basement. The surface extension of the subsurface vertical is shown with a long dash line in Fig. 9. The two parallel, south-dipping reflectors highlighted in Fig. 5 are clearly intersected by the main branch of the North Anatolian Fault. En échelon segments to the south of the North Anatolian Fault are seen to be very recent, documenting their continued activity. En échelon tension fractures may form along a strike-slip faulting zone in the initial stage of deformation, but they are easily destroyed as strike-slip displacement increases and compressive structures became more prominent (Wilcox et al. 1973). Furthermore, a mud volcano seen in both bathymetry and seismic sections around the en échelon faults, as well as the acoustically transparent character of seismic sections may indicate the presence of gas. Mud volcanoes in that area, as well as shallow gas-charged sediments, were recognized and described by Cormier et al. (2006).

Central Basin

In the central basin, the northern branch of the North Anatolian Fault is observed in almost all the seismic sections, with very similar seismic characters forming a vertical discontinuity from sea bottom to at least 0.5 s two-way travel times (Fig. 7). The steep main fault separates two different stratigraphic units parallel to sub-parallel sediments to the south and folded strata to the north. These units are bordered by two normal faults in seismic Sect. 25. E–W trending, normal secondary faults are associated with the two border faults. Cormier et al. (2006) interpreted these small, shallow-rooted faults as the result of marginal mass wasting, because in map view, based on high-resolution multibeam bathymetry, they display short lateral extent (about 1 km, up to 2 km) and wavy shapes. Alpar and Yaltırak (2002) pointed out that the main fault in the gulf has a negative flower structure, but their interpretation of the main fault strand is displaced toward the southern coast of the central basin. They were not able to see the deeper part of the sections showing the strike-slip character of the fault because of the limited penetration of their single-channel seismic data. In our study, the two border fault systems converge in the deeper part of the seismic section, giving the fault system a negative flower structure geometry. The ENE-WSW trending right-lateral oblique Karamürsel Fault extends along the southern coast of the central basin (Alpar and Yaltırak 2002). The central basin is thus limited by the Karamürsel Fault to the south, extrapolated on seismic Sect. 25 from the southern onshore

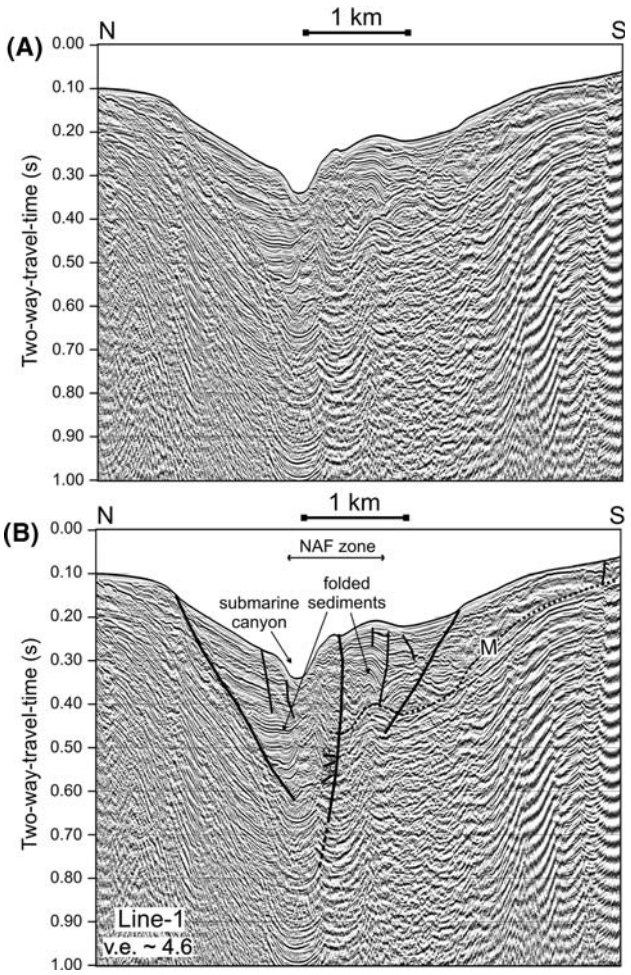

Fig. 10 **a** Time-migrated seismic Section-1. **b** Interpreted section. The section shows the vertical discontinuity as NAF, north and south border faults around the NAF and folded sediments at each side of the fault. *M* sea bottom multiple, *v.e* vertical exaggeration

(Fig. 7). The basement is expected to be composed of units of Paleozoic metamorphic rocks as exposed on the Armutlu Peninsula (Okay et al. 1994).

There are two subsidiary troughs, lenticular in plan view and trending E–W with maximum depth of 205 m in the central basin. The North Anatolian Fault has a dip-slip component following the northern border of these troughs. Yet, between the troughs the fault has purely strike-slip component (Figs. 7, 9). The pure strike-slip character of the fault is observed on Sects. 25–28, separating two different seismic units on each side. The fault surface here is near vertical without vertical motion. However, other studies relying on high-resolution shallow-penetration seismic sections propose that the main fault is located north of where we interpret it to be (Kuşçu et al. 2002; Cormier et al. 2006). Based on our deeper penetrating seismic data, we argue instead that the fault trace actually follows the southern side of the folded structures (Fig. 11). Cormier et al. (2006) mapped these folds as en échelon folds trending NNE-SSW. On the other hand, to the north of the northern border fault, relatively smaller scale folded units are not directly formed by tectonic movements.

Cormier et al. (2006) define the lumpy texture around the basin periphery as being preferentially formed by mass wasting and fluidization of gas-charged sediments, probably induced by earthquake events. However, these are not surficial features affecting only the upper Holocene drape as described by Cormier et al. (2006). Their continuity can now be followed to the deeper levels in our sections. Their folded and faulted nature is attributable to their sliding on the 20° south-dipping Paleozoic basement because of gravitational forces and subsidence along the main and/or secondary faults.

Sediments are thickest in the deepest part of the central basin. To the south of the North Anatolian Fault the seismic sequences are classified according to their seismic characteristics (Fig. 11). The upper unit (T3) is characterized by low seismic amplitude or an absence of internal reflectors. A major erosional surface is observed near the base of stratigraphic Unit T3 (Fig. 11). To the north, older sedimentary units are truncated by an unconformity surface below unit T3 (Figs. 7, 11). The Gulf of İzmit was a lacustrine environment as part of a "Marmara Lake" during the late glaciation and early deglaciation until ~12 ka, when the Marmara Basin was inundated by Mediterranean waters (Çağatay et al. 2003). In this scenario, the uppermost unit (T3) would represent the Holocene marine sediments with a maximum thickness of 19 m. The main branch of the North Anatolian Fault cuts these sediments in the deeper part of basin (inset of Fig. 11).

The lower two units (Units T2 and T1) are separated by an erosional surface and can be correlated with the Marmara formation. The Marmara formation has a regressive to transgressive character and includes units of middle to upper Pleistocene (Alpar and Yaltırak 2002). The thicknesses of Units T2 and T1 against the fault trace are 83 and 158 m, respectively. Maximum sedimentation rates can be calculated according to the unconformity ages of the Marmara formation. Unconformity ages at the base of the two units of the Marmara formation are 130 and 600 ka, as derived from the generalized stratigraphic section of the study area (Alpar and Yaltırak 2002; Fig. 3b). According to Alpar and Yaltırak (2002), unconformity ages of these two units are given by comparing with global sea-level curves (Chappell and Shackleton 1986) and radiometric ages of coastal terrenes along Strait of Çanakkale (Dardanalles) (Yaltırak et al. 2000, 2002). As a result, sedimentation rates for Units T3, T2 and T1 are 1.6 mm/year (=19 m/(24–12) ka), 0.8 mm/year (=83 m/(130–24) ka) and 0.3 mm/year (=158 m/(600–130) ka), respectively. The overall average sedimentation rate is calculated as 0.4 mm/year (260 m/600 ka).

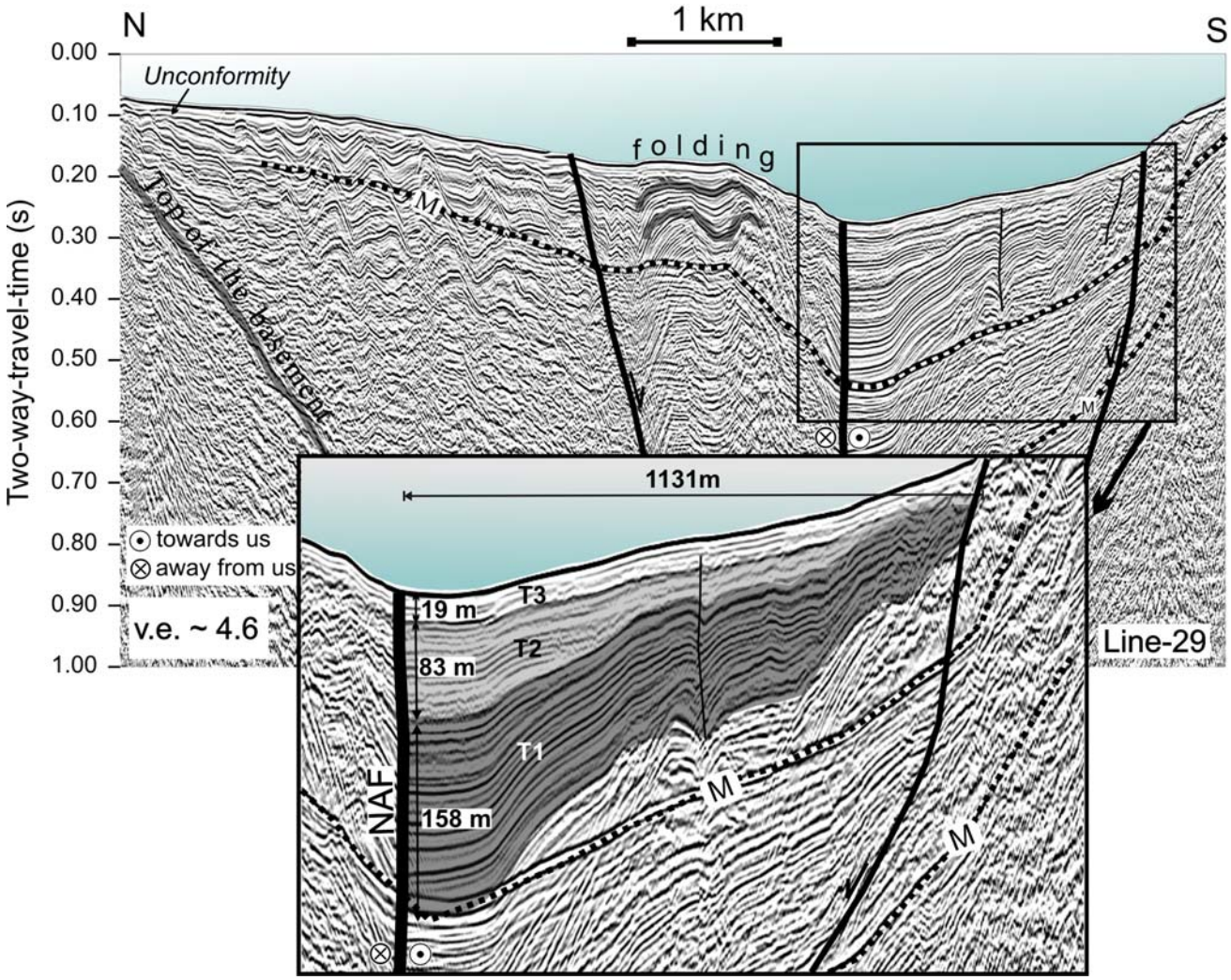

Fig. 11 Interpreted time-migrated seismic Section-29 and enlarged area of the same section. Three stratigraphic units (T1, T2, and T3) of the NAF are defined according to their seismic characters

Eastern Basin

The eastern part of the gulf has a relatively shallow and flat bathymetry. Two main groups of sub-parallel faults are observed on seismic sections and are well correlated with the lineaments observed in the multibeam bathymetry (Fig. 8). Strong sea bottom multiples caused by the shallow bathymetry make it difficult to observe the fault geometry in the deeper parts of the section. Nevertheless, older studies follow the main fault zone through the high-resolution shallow seismic sections and they draw the main fault orientation in a NW-SE direction (Alpar and Yaltırak 2002; Kuşçu et al. 2002). North Anatolian Fault enters the gulf in an E–W direction through the eastern basin. The NW-SE orientation and south-dipping normal component on the faults suggests that this section of the North Anatolian Fault may contain a releasing bend. Alternatively, the two parallel faults in the basin can be considered to be Riedel faults of the E–W trending North Anatolian Fault in the eastern trough of the gulf. In our seismic sections, these two faults are seen to be identical and we interpret these two main groups of faults as forming a fault zone within the North Anatolian Fault. Moreover, the presence of gas-charged sediments and several gas plumes in the water column related to these faults were detected in the eastern gulf using high-resolution seismic data acquired in 2000 (Kuşçu et al. 2005).

Conclusions

The main branch of the dextral North Anatolian Fault enters the Gulf of İzmit from its eastern part and crosses the gulf mainly in an E–W direction and connects to deep troughs of the Sea of Marmara in the west. The fault causes an active tectonic stratigraphic setting for the Gulf of İzmit

and it mainly forms a nearly vertical fault surface from sea bottom to about 1,000 m depth. The overall average sedimentation rate is 0.4 mm/year according to the three youngest seismo-stratigraphic units located to the south of the main fault branch within the central basin. The top of Paleozoic basement is extended along the northern shoreline of the gulf with a 20° south-dipping angle.

Acknowledgments We thank the captain and the crew of the R/V MTA Sismik-1 for their efforts during data acquisition. We also thank İsmail Kuşçu, Kerim Sarıkavak and Füsun Öcal for their help in providing seismic data. We appreciate the Department of Navigation, Hydrography and Oceanography of the Turkish Navy (SHOD) for providing eastern basin bathymetric data. The maps were produced by GMT software package (Wessel and Smith 1998). Focus (5.0) is used for seismic processing, thanks to Paradigm Geophysical for free updates. We thank Dr. Onur Tan for computational matters and Dr. Berkan Ecevitoğlu for the contribution to the seismic data collection and processing. Special thanks to Dr. Emin Demirbağ, Dr. Marie-Helene (Milene) Cormier, Dr. Christopher Sorlien, Dr. Okan Tüysüz, Dr. Leonardo Seeber, Dr. Namık Çağatay, Dr. Cenk Yaltırak and Dr. Luca Gasperini for their valuable constructive discussions. Comments and constructive reviews by anonymous referees and Editor in Chief Dr. Peter Clift are gratefully acknowledged. Istanbul Technical University Research Project funded this study.

References

Alpar B, Yaltırak C (2002) Characteristic features of the North Anatolian Fault in the eastern Marmara region and its tectonic evolution. Mar Geol 190:329–350. doi:10.1016/S0025-3227(02)00353-5

Barka A (1996) Slip distribution along the North Anatolian Fault associated with the large earthquakes of the period 1939–1967. Bull Seism Soc Am 86:1238–1254

Barka A (1997) Neotectonics of the Marmara region in active tectonics of Northwest Anatolia. In: Schindler C, Pfister M (eds) The Marmara poly-project. Hochschulverlag AG an der ETH, Zurich, pp 55–87

Barka A (1999) The 17 August 1999 İzmit earthquake. Science 285:1858–1859. doi:10.1126/science.285.5435.1858

Çağatay MN, Görür N, Polonia A et al (2003) Sea-level changes and depositional environments in the İzmit Gulf, eastern Marmara Sea, during the late glacial–Holocene period. Mar Geol 202:59–173. doi:10.1016/S0025-3227(03)00259-7

Chappell J, Shackleton NJ (1986) Oxygen isotopes and sea level. Nature 324:137–140. doi:10.1038/324137a0

Cormier MH, Seeber L, McHugh CMG et al (2006) North Anatolian Fault in the Gulf of Izmit (Turkey): rapid vertical motion in response to minor bends of a nonvertical continental transform. J Geophys Res Solid Earth 111(B4):1–25. doi:10.1029/2005jb003633

Emre Ö, Erkal T, Tchepalyga A et al (1998) Neogene-quaternary evolution of the Eastern Marmara region, Northwest Turkey. Bull Min Res Explor Inst Turk 120:119–145

Emre Ö, Awata Y, Duman TY (2003) Surface rupture associated with the 17 August 1999 Izmit earthquake. Gen Dir of Miner Res and Explor, Ankara, p 280

Gökaşan E, Alpar B, Gazioğlu C et al (2001) Active tectonics of the İzmit Gulf (NE Marmara Sea): from high resolution seismic and multi-beam bathymetry data. Mar Geol 175:273–296. doi:10.1016/S0025-3227(01)00133-5

Kuşçu İ, Okamura M, Matsuoka H et al (2002) Active faults in the Gulf of İzmit on the North Anatolian Fault, NW Turkey: a high-resolution shallow seismic study. Mar Geol 190:421–443. doi:10.1016/S0025-3227(02)00357-2

Kuşçu İ, Okamura M, Matsuoka H et al (2005) Seafloor gas seeps and sediment failures triggered by the August 17, 1999 earthquake in the Eastern part of the Gulf of İzmit, Sea of Marmara, NW Turkey. Mar Geol 215:193–214. doi:10.1016/j.margeo.2004.12.002

Okay AI, Şengör AMC, Görür N (1994) Kinematic history of the opening of the Black Sea and its effect on the surrounding regions. Geology 22:267–270. doi:10.1130/0091-7613(1994)022<0267:KHOTOO>2.3.CO;2

Okyar M, Pınar A, Tezcan D et al (2008) Late quaternary seismic stratigraphy and active faults of the Gulf of İzmit (NE Marmara Sea). Mar Geophys Res 29:89–107. doi:10.1007/s11001-008-9049-6

Parsons T, Toda S, Stein R et al (2000) Heightened odds of large earthquakes near Istanbul: an interaction-based probability calculation. Science 228:661–665. doi:10.1126/science.288.5466.661

Polonia A, Gasperini L, Amorosi A et al (2004) Holocene slip rate of the North Anatolian Fault beneath the Sea of Marmara. Earth Planet Sci Lett 227:411–426. doi:10.1016/j.epsl.2004.07.042

Şaroğlu F (1988) Age and pure offset of the North Anatolian Fault. Middle East Tech Univ J Pure Appl Sci 21:65–79

Şengör AMC, Görür N, Şaroğlu F (1985) Strike-slip faulting and related basin formation in zones of tectonic escape: Turkey as a case study. In: Biddle KT, Christie-Blick N (eds) Strike-slip deformation, basin formation and sedimentation. Soc Econ Paleontol Mineral Spec Publ, vol. 37:pp 227–264

Şengör AMC, Demirbağ E, Tüysüz O, et al. (1999) A preliminary note on the structure of the Gulf of Izmit: implications for the westerly prolongation of the North Anatolian Fault. In: Proceedings of the İTU-IAHS International conference on the Kocaeli earthquake, İstanbul, pp 25–37

Stein RS, Barka A, Dieterich JH (1997) Progressive failure on the North Anatolian Fault since 1939 by earthquake stress triggering. Geophys J Int 128:594–604. doi:10.1111/j.1365-246X.1997.tb05321.x

Sylvester AG (1988) Strike-slip faults. Geol Soc Am Bull 100:1666–1703. doi:10.1130/0016-7606(1988)100<1666:SSF>2.3.CO;2

Taymaz T (1999) Seismotectonics of the Marmara region: source characteristics of 1999 Gölcük-Sapanca-Düzce earthquakes. In: Proceedings of the İTU-IAHS International conference on the Kocaeli earthquake, İstanbul, pp 55–78

Tchalenko JS (1970) Similarities between shear zones of different magnitudes. Geol Soc Am Bull 81:1625–1640. doi:10.1130/0016-7606(1970)81[1625:SBSZOD]2.0.CO;2

Wernike B, Burchfiel BC (1982) Modes of extensional tectonics. J Struct Geol 4:105–115. doi:10.1016/0191-8141(82)90021-9

Wessel P, Smith WHF (1998) New improved version of Genetic Mapping Tools released. Eos Trans AGU 79:579. doi:10.1029/98EO00426

Wilcox RE, Harding TP, Seely DR (1973) Basic wrench tectonics. Am Assoc Pet Geol Bull 57:74–96

Yaltırak C, Alpar B, Sakınç M et al (2000) Origin of the strait of Canakkale (Dardanelles): regional tectonics and the Mediterranean–Marmara incursion. Mar Geol 164:139–156. doi:10.1016/S0025-3227(99)00134-6

Yaltırak C, Sakınç M, Aksu AE et al (2002) Late Pleistocene uplift history along southwestern Marmara Sea determined from raised coastal deposits and global sea level variations. Mar Geol 190:283–305. doi:10.1016/S0025-3227(02)00351-1